Inorganica Chimica Acta 408 (2013) 84–90

Contents lists available at ScienceDirect

Inorganica Chimica Acta

journal homepage: www.elsevier.com/locate/ica

Syntheses, crystal structures and properties of five divalent transition metal coordination compounds based on a semirigid tetracarboxylic acid ligand

Meihui Yu, Ming Hu *, Zhenting Wu, Haiquan Su *

Inner Mongolia Key Laboratory of Chemistry and Physics of Rare Earth Materials, School of Chemistry and Chemical Engineering, Inner Mongolia University, Hohhot 010021, PR China

ARTICLE INFO

Article history:
Received 26 April 2013
Received in revised form 27 July 2013
Accepted 27 August 2013
Available online 5 September 2013

Keywords:
Coordination compounds
Semirigid ligand
Crystal structure
Photoluminescence
Magnetic property

ABSTRACT

Five divalent transition metal coordination compounds based on a semirigid tetracarboxylic acid have been synthesized by the hydrothermal method, namely, $[MnL_{0.5}phen]_n$ (**1**), $[CdL_{0.5}phen]_n$ (**2**), $[Co(H_2L)(phen)_2H_2O]_n$ (**3**), $\{[Ni_2L(phen)_2(H_2O)_6]\cdot 2H_2O\}_n$ (**4**) $\{[Zn_2L(phen)_4(H_2O)_2]\cdot 2H_2O\}_n$ (**5**) (H_4L = 1,4-bis(4-oxy-1,2-benzene dicarboxylic acid)benzene, phen = 1,10-phenanthroline). These compounds were structurally characterized by infrared spectra, thermogravimetric analyses and single crystal X-ray diffractions. The isostructural **1** and **2** exhibit the two-dimensional layered structures. Compound **3** and **4**–**5** reveal a mononuclear and two dinuclear structures, respectively. In addition, the magnetic property of **1** and the photoluminescence of **2** and **5** were also investigated, respectively.

1. Introduction

Numbers of the researches in supramolecular chemistry and crystal engineering have focused on the rational design and synthesis of multifunctional metal–organic frameworks (MOFs) in the past decade [1]. MOFs have been attracted much attentions for their fascinating architectures and potential applications in the fields of gas adsorption and storage, ion exchange, catalysis, molecular magnetism and photoluminescence [2,3]. A considerable amount of coordination polymers with interesting structures and well-established topologies have been successfully synthesized, such as metal-carboxylates MOFs based on d-block transition and lanthanide metal ions [4,5]. In the process of building coordination polymers, some factors must be considered for the design of constructions, such as the length and flexibility of ligands, the coordination modes of the metal ions and the pH of reaction system [6–12]. The researches about the rigid and semirigid multicarboxylate ligands are still good candidates for building MOFs, which can be attributed to the rich varieties of coordination modes of multicarboxylate groups [13,14].

In contrast to the rigid ligands with difficult conformational changes in the assembly of coordination polymers, the semirigid ligands can easily regulate its configurations to enhance the structural diversity. On the other hand, the semirigid ligands have also been proved to be efficient building blocks in the construction of various dimensional coordination polymers [15,16]. In addition, an effective and controllable route is to introduce auxiliary rigid multidentate N-donor ligands. However, less studies about both semirigid carboxylate ligands and auxiliary multidentate N-donor ligands have been reported [17–21].

Herein, we select a semirigid ligand attached four carboxylate groups in symmetrical positions, namely, 1,4-bis(4-oxy-1,2-benzene dicarboxylic acid)benzene (H_4L). H_4L is a long tetracarboxylate ligand with two semirigid –O– spatial linkers, which can impart a variety of connection modes with metal centers and generate abundant structural motifs [22]. Meanwhile, H_4L can bond and rotate along two semirigid –O– spacer so that it improves the coordination ability and the structural peculiarity when it coordinates to metal centers. In this paper, we have prepared five transition metal coordination compounds using the semirigid H_4L by the hydrothermal method, the structures, thermal stabilities, luminescent and magnetic properties of some complexes were explored in detail.

2. Experimental

2.1. Materials and general methods

The 1,4-bis(4-oxy-1,2-benzene dicarboxylic acid)benzene was synthesized according to the literature procedure [23]. All other reagents were used as received from commercial sources without

---

* Corresponding authors. Tel.: +86 0471 4992981.
E-mail address: hm988@126.com (M. Hu).

0020-1693/$ - see front matter © 2013 Elsevier B.V. All rights reserved.
http://dx.doi.org/10.1016/j.ica.2013.08.022

further purification. Elemental analyses (C, H and N) were determined on Perkin-Elmer 2400 analyzer. The IR spectra were recorded as KBr pellets on a Nicolet Avatar-360 spectrometer in the 400–4000 cm^{-1} region. Thermogravimetric analysis (TGA) was performed on a Perkin-Elmer TG-7 analyzer heated from 25 to 800 °C under air atmosphere. Powder X-ray power diffraction (PXRD) was performed on a X'Pert PRO (PW3071/xx Bracket) diffractometer with Cu Kα radiation (λ = 1.5406 Å). The fluorescent spectra were measured on a FLS920 spectrophotometer.

2.2. Synthesis of complexes **1**–**5**

2.2.1. Synthesis of complex $[MnL_{0.5}phen]_n$ (**1**)

A mixture of $MnCl_2 \cdot 4H_2O$ (0.2 mmol, 39.6 mg), H_4L (0.1 mmol, 43.8 mg), phen (0.2 mmol, 39.6 mg) and H_2O (12 mL) was stirred for 30 min at room temperature and was sealed in a 23 mL Teflon-lined stainless steel vessel, heated at 160 °C for 72 h, kept 20 h at 100 °C and followed by slow cooling to the room temperature at a rate of 5 °C h^{-1}. The faint yellow crystalline product was obtained, isolated by filtration, then washed with H_2O and air-dried, yield 61%. IR (KBr pellet): 3416.89(s), 1626.07(s), 1492.52(m),1395.14(s), 1259.36(m), 1216.01(s), 1188.37(w), 842.73(m), 725.53(m). *Anal.* Calc. for **1**: C, 61.08; H, 2.90; N, 6.20. Found: C, 61.04; H, 2.87; N, 6.23%.

2.2.2. Synthesis of complex $[CdL_{0.5}phen]_n$ (**2**)

Complex **2** was synthesized in a similar procedure to that described for **1** with the exception that $Cd(NO_3)_2 \cdot 4H_2O$ (0.2 mmol, 61.7 mg) was replaced by $MnCl_2 \cdot 4H_2O$ and 15 mL H_2O. The colorless crystal of **2** was collected, washed with H_2O, and air-dried. Yield 55%. IR (KBr pellet): 3432.33(s), 1665.94(w), 1571.58(m), 1492.27(s), 1374.57(s), 1272.75(m), 1216.98(s), 1183.00(m), 844.43(m), 769.60(m). *Anal.* Calc. for **2**: C, 54.19; H, 2.58; N, 5.50. Found: C, 54.01; H, 2.61; N, 5.48%.

2.2.3. Synthesis of complex $[Co(H_2L)(phen)_2H_2O]_n$ (**3**)

The method of synthesis was similar to that used for **2** with the exception that $Co(NO_3)_2 \cdot 6H_2O$ (0.2 mmol, 58.2 mg) was instead of $Cd(NO_3)_2 \cdot 4H_2O$. The orange crystal of **3** was collected, washed with H_2O and air-dried. Yield 57%. IR (KBr pellet): 3419.65(s), 1607.24(s), 1544.58(s), 1412.03(s), 1255.45(m), 1227.72(s), 1192.32(m), 814.46(m). *Anal.* Calc. for **3**: C, 63.23; H, 3.47; N, 6.4. Found: C, 63.25; H, 3.45; N, 6.37%.

2.2.4. Synthesis of complex $\{[Ni_2L(phen)_2(H_2O)_6] \cdot 2H_2O\}_n$ (**4**)

The method of synthesis was similar to that used for **2** with the exception that $NiSO_4 \cdot 6H_2O$ (0.2 mmol, 52.6 mg) was instead of $Cd(NO_3)_2 \cdot 4H_2O$. The faint blue crystal of **4** was collected, washed with H_2O and air-dried. Yield 52%. IR (KBr pellet): 3439.08(s), 1630.57(s), 1493.17(m), 1424.38(s), 1259.93(m), 1218.97(s), 1184.60(m), 847.82(s), 726.25(s). *Anal.* Calc. for **4**: C, 52.31; H, 4.02; N, 5.31. Found: C, 52.28; H, 4.00; N, 5.29%.

2.2.5. Synthesis of complex $\{[Zn_2L(phen)_4(H_2O)_2] \cdot 2H_2O\}_n$ (**5**)

A mixture of $Zn(NO_3) \cdot 6H_2O$ (0.2 mmol, 59.5 mg), H_4L (0.1 mmol, 43.8 mg), phen(0.2 mmol, 39.6 mg) in 15 mL of mixed H_2O-C_2H_5OH-NaOH (0.1 mmol/mL) (9:2:4,v/v/v) was placed in a 23 mL Teflon-lined stainless steel vessel, heated at 160 °C for 72 h, kept 20 h at 100 °C, and then followed by slow cooling to the room temperature at a rate of 5 °C h^{-1}. The colorless crystal of **5** was collected, washed with H_2O, and air-dried. Yield 50%. IR (KBr pellet): 1682.37(s), 1588.06(m), 1500.83(w), 1433.47(m), 1301.15(s), 1188.39(m), 943.92(m), 721.81(s). *Anal.* Calc. for **5**: C, 61.86; H, 3.68; N, 8.25. Found: C, 61.85; H, 3.66; N, 8.24%.

2.3. X-ray crystallography

Crystallographic data for compounds **1**–**5** were collected on a Bruker Apex Smart CCD diffractometer with graphite-monochromated Mo Kα radiation (λ = 0.71073 Å) using the ω-scan technique at room temperature. All the structures were solved by direct methods with SHELXS-97 and refined with the full-matrix least-squares $|F|$ [2] technique using the SHELXL-97 [24] program. The position of non-hydrogen atoms were refined with anisotropic displacement parameters. The hydrogen atoms were set in calculated positions and refined as riding atoms with a common isotropic thermal parameter. The crystallographic data for **1**–**5** are listed in Table 1. The selected bond lengths and angles of **1**–**5** are listed in Tables S1–S5.

Table 1
The crystallographic data for complexes **1**–**5**.

Compound	1	2	3	4	5
Formula	$C_{23}H_{13}MnN_2O_5$	$C_{23}H_{13}CdN_2O_5$	$C_{46}H_{30}CoN_4O_{11}$	$C_{46}H_{42}Ni_2N_4O_{18}$	$C_{70}H_{50}Zn_2N_8O_{14}$
Formula weight	452.29	509.75	873.67	1056.22	1357.96
T (K)	293(2)	293(2)	293(2)	293(2)	293(2)
Crystal system	monoclinic	monoclinic	monoclinic	triclinic	triclinic
Space group	$P2_1/c$	$P2_1/c$	$P2_1/c$	$P\bar{1}$	$P\bar{1}$
a (Å)	7.0841(3)	7.1818(9)	13.4288(9)	7.3598(9)	10.1243(6)
b (Å)	18.3818(7)	18.432(3)	15.5207(11)	12.5630(9)	11.8713(8)
c (Å)	14.8668(6)	14.9225(18)	20.4934(17)	13.3038(15)	13.1068(11)
α (°)	90.00	90.00	90.00	70.312(8)	83.565(6)
β (°)	96.280(4)	96.818(12)	114.856(6)	78.188(10)	68.614(7)
γ (°)	90.00	90.00	90.00	87.863(7)	79.565(5)
V (Å^3)	1924.32(13)	1961.4(5)	3875.7(5)	1133.0(2)	1440.74(19)
Z	4	4	4	1	1
D_{cal}(g cm^{-3})	1.561	1.726	1.497	1.548	1.565
μ (mm^{-1})	0.726	1.153	0.515	0.914	0.914
F(000)	920	1012	1796	546	698
R_{int}	0.0478	0.1201	0.0658	0.0425	0.0306
Goodness-of-fit (GOF)	1.043	1.011	1.016	1.049	1.054
R_1[a]	0.0399	0.0552	0.0476	0.0511	0.0346
ωR_2[b] $[I > 2\sigma(I)]$	0.0726	0.1262	0.0896	0.1126	0.0785
R_1 (all data)	0.0626	0.1089	0.0836	0.0741	0.0413
wR_2 (all data)	0.0812	0.1821	0.1053	0.1287	0.0833

[a] $R_1 = \sum||F_o| - |F_c||/\sum|F_o|$.
[b] $\omega R_2 = [\sum[\omega(F_o^2 - F_c^2)^2]/\sum\omega(F_o^2)^2]^{1/2}$.

3. Results and discussion

3.1. Structural description of $[MnL_{0.5}phen]_n$ (**1**)

Complex **1** crystallizes in the monoclinic system with space group $P2_1/c$. There are one Mn(II) ion, a half of L^{4-} and one phen molecule in the asymmetric unit of **1**. The coordination environment and atom connectivity for **1** are shown in Fig. 1a. Mn(II) ion is six-coordinated with a distorted octahedron geometry, which is coordinated by four O atoms (O1, O3, O2#2, and O4#1) of monodentate carboxylate groups from three ligands and two nitrogen atoms (N1, N2) from phen. All carboxylate groups of each H_4L ligand link neighboring Mn(II) ions in the the mode of μ_2-η^1:η^1 (Scheme 1a). The Mn–O bond distances range from 2.1411(19) to 2.2402(19) Å; the Mn–N bond lengths of 2.297(2) and 2.309(2) Å are slightly longer than that of Mn–O, which are well-matched to those observed in the reported complexes [25]. Every two crystallographically equivalent Mn(II) ions are bridged by two carboxylate groups to obtain a binuclear building block. The building blocks are connected each other through carboxylate groups along *a* axis to lead to a one-dimensional (1D) infinite zigzag chain (Fig. 1b). The adjacent 1D chains are further linked by the carboxylate oxygen atoms to generate a 2D layer viewed along the *b* axis (Fig. 1c). The distances between two adjacent Mn^{2+} ions in a zigzag chain which are linked by the carboxylate groups are 4.2988 and 4.8516 Å, respectively, and the distance of Mn^{2+} ions between two adjacent chains which are linked by the carboxylate groups is 9.8312 Å. At the same time, there are weak π–π interactions between pyridyl rings of phen and those of the phenyl rings, the distance of centroids is 3.9709 Å [26]. The Mn(II) ions and the L^{4-} ligands can be considered as 3-connected and 6-connected nodes, respectively, in which Mn(II) ions are represented with the point (Schlafli) symbol $\{4^3\}$ and the ligands with the point (Schlafli) symbol $\{4^6.6^6.8^3\}$. The structure can be simplified as 3,6-connected framework with the point (Schlafli) symbol $\{4^3\}_2\{4^6.6^6.8^3\}$ (Fig. 1d).

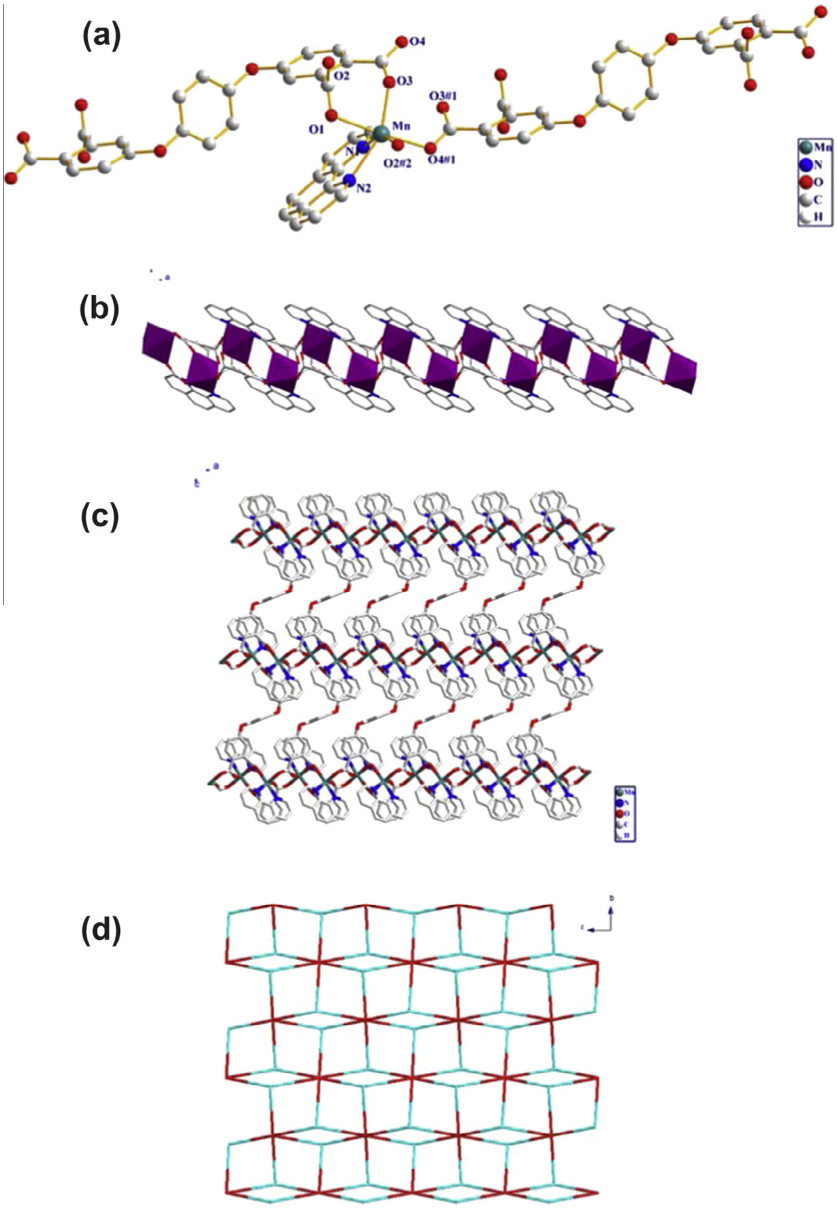

Fig. 1. (a) Coordinated environment of Mn(II) ion (symmetry codes: #1 $-x+2, -y, -z$; #2 $-x+1, -y, -z$); (b) A view showing a 1D chain running along the *a* axis; (c) A view of the 2D sheet by L^{4-} ligand and Mn(II) along the *b* axis; (d) The topology of 1 (red and blue balls represent 6-connected L^{4-} ligands and 3-connected Mn(II), respectively).

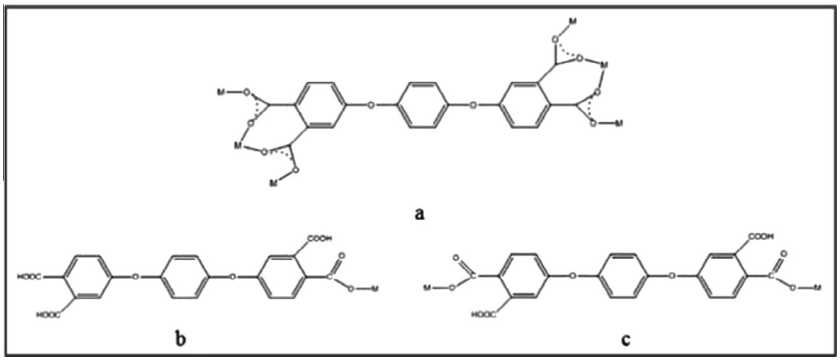

Scheme 1. Coordination modes of H_4L (1,4-bis(4-oxy-1,2-benzene dicarboxylic acid)benzene).

3.2. Structural description of $[CdL_{0.5}phen]_n$ (**2**)

Compound **2** is isostructural to **1**. As shown in Fig. S1a and c, the coordinated environment and the topology of 2 are identical to those of 1. The Cd–O and Cd–N bond lengths range from 2.235(5) to 2.399(6) Å and 2.375(7) to 2.395(7) Å, respectively, which are similar to those observed in the reported complexes.[27b].

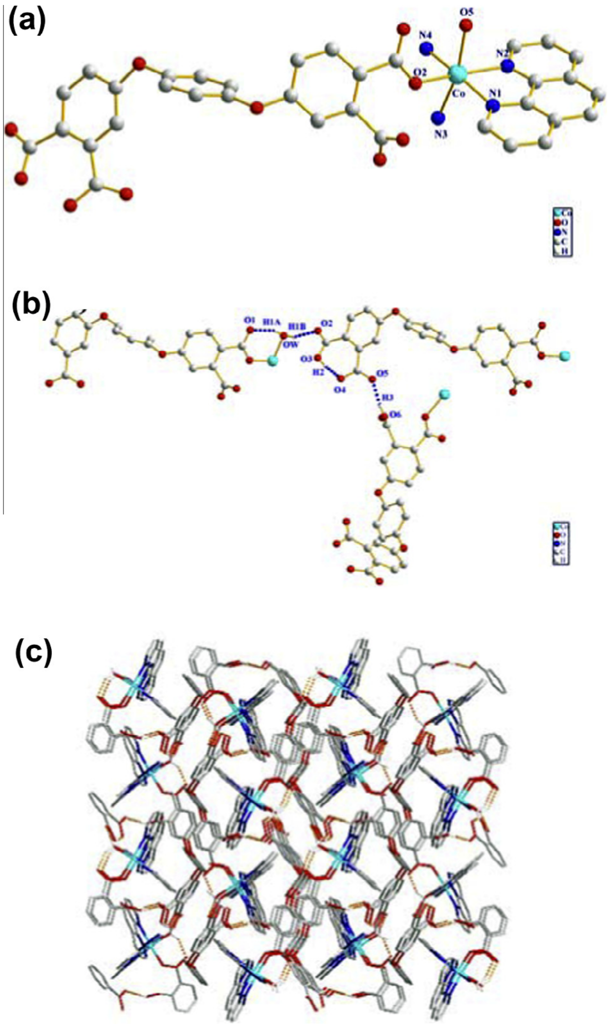

Fig. 2. (a) Coordinated environment of Co(II) ion. (b) The modes of hydrogen bonds. (c) The 3D supramolecular architecture of compound **3**.

3.3. Structural description of $[Co(H_2L)(phen)_2H_2O]_n$ (**3**)

Compound **3** crystallizes in the monoclinic system with $P2_1/c$ space group. In the asymmetric unit of $[Co(H_2L)(phen)_2H_2O]$, there are one Co(II) ion, one partly deprotonated H_2L^{2-} ligand, two auxiliary ligands phen and one coordinated water molecule. The six-coordinated Co(II) ion is surrounded by a monodentate carboxylate group from the H_2L ligand, four nitrogen atoms from two phen, and one oxygen atom from the water molecule (Fig. 2a). The Co–O bond distances are 2.046(2) and 2.095(2) Å, respectively, and the Co–N bond lengths ranges from 2.133(2) to 2.172(3) Å, which are similar to the reported Co–O and Co–N bond distances [27]. The bond angles around the Co(II) center are in the range of 77.57(9)°–168.12(10)°. The carboxylate groups of ligands show monodentate mode to link one Co(II) ion (Scheme 1b) to form a mononuclear unit. The different units are connected by two kinds of intermolecular hydrogen bonds. The detailed modes of hydrogen bonding are shown in Fig. 2b, (Supporting information, Table S6). Then, the mononuclear units are combined through the intermolecular hydrogen bonds to form a 3D supramolecular structure (Fig. 2c).

3.4. Structural description of $\{[Ni_2L(phen)_2(H_2O)_6]\cdot 2H_2O\}_n$ (**4**)

Complex **4** crystallizes in the triclinic system with $P\bar{1}$ space group. In the dinuclear structure of **4**, the symmetric unit is composed of two Ni(II) ions, one totally deprotonated L^{4-} ligand, two phen, six coordinated and two lattice water molecules. Each Ni(II) ion is six-coordinated with a slight distorted octahedron environment by a carboxylate oxygen atom from ligand, two nitrogen atoms from phen, and three terminal water molecules (Fig. 3a). The carboxylate groups of ligands show monodentate mode to link two Ni(II) ions (Scheme 1c). The Ni–O and Ni–N bond lengths range from 2.006(3) to 2.138(3) Å, 2.069(3) to 2.071(3) Å, respectively; the distance between two Ni(II) ions is 19.665 Å. The bond angles around Ni(II) center range in 80.43(12)°–178.70(12)°. There are existing hydrogen-bonding including intramolecular and intermolecular interactions, which are formed between water molecules and carboxylate oxygen atoms (Supporting information, Table S7,). In the formation of hydrogen bondings, the uncoordinated carboxylate oxygen atoms act fully as proton acceptors. Finally, the dinuclear units are extended to a 3D supramolecular architecture by intermolecular hydrogen-bonding interactions (Fig. 3b).

3.5. Structural description of $\{[Zn_2L(phen)_4(H_2O)_2]\cdot 2H_2O\}_n$ (**5**)

Compound **5** has a triclinic space group $P\bar{1}$ and also exhibits a dinuclear structure, and the symmetric unit of 5 contains two Zn(II) ions, one L^{4-} anion ligand, four phen, two coordinated and

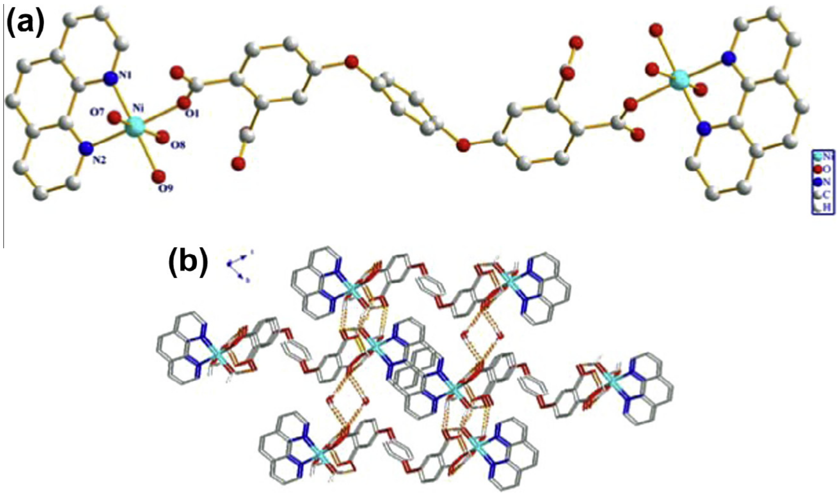

Fig. 3. (a) Coordinated environment of Ni(II) ion. (b) The 3D supramolecular architecture of **4**.

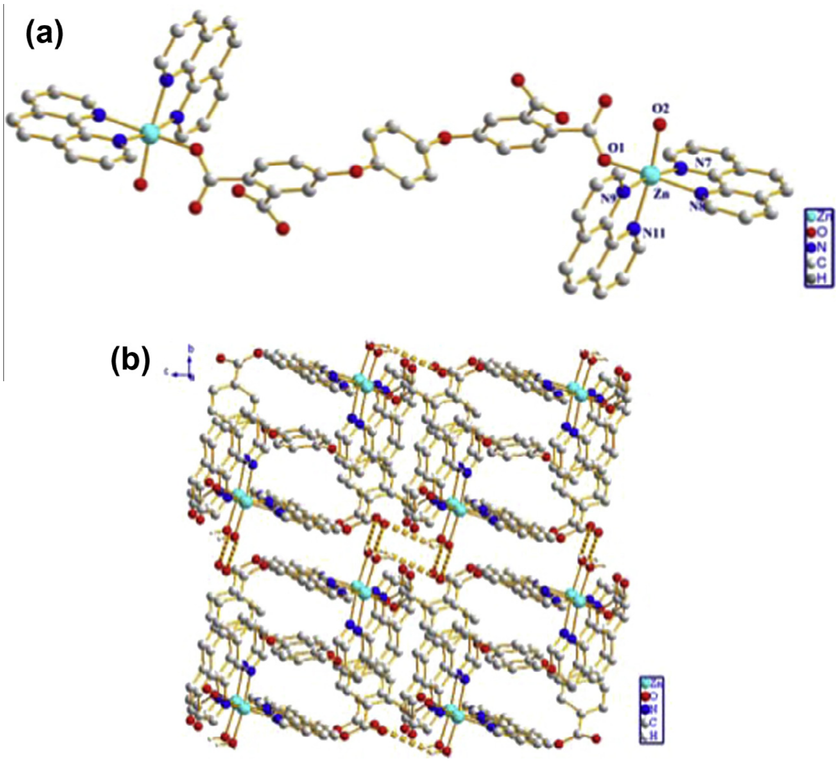

Fig. 4. (a) Coordinated environment of Zn(II) ion. (b) The 3D supramolecular architecture of 5.

two lattice water molecules. As shown in Fig. 4a, each Zn(II) ion is six coordinated by a carboxylate oxygen atom from L^{4-} ligand (Zn–O 2.0976(18) Å), four nitrogen atoms from two phen molecules, and one terminal water molecule (Zn–O 2.0673(18) Å), which forms a slight distorted octahedron. The bond lengths of Ni–N range from 2.156(2) to 2.210(2) Å, and the distance between two Zn(II) ions is 19.24 Å in symmetric unit. The bond angles around Zn(II) center are between 76.89(8)° and 172.00(7)°. The two central Zn(II) ions are connected each other through a L^{4-} anion, which forms a dinuclear structural unit. The carboxylate groups of ligands show monodentate mode to link two Zn(II) ions (Scheme 1c). Then, the dinuclear units are combined through the intermolecular hydrogen bonds, which are composed of water molecules and uncoordinated carboxylate oxygen atoms and finally formed a 3D supramolecule (Fig. 4b) (Supporting information, Table S8).

3.6. Thermogravimetric analysis and PXRD

Compounds **1**–**5** were detected with a heating rate of 5 °C/min in the range of 25–800 °C under the air atmosphere (Fig. S2). Compound **1**–**2** maintain a considerable thermal stability up to the temperature of 360 and 300 °C, respectively. The TGA curve of **1** exhibits that the weight loss above 360 °C stems from the decomposition of frameworks. For **2**, the firstly weight loss is observed from 300 to 530 °C, which is attributed to the loss of the a phen, the L^{4-} ligands are secondly removed from the complex during

530–730 °C, with the decomposition of frameworks of **2**. For **3**, the first weight loss from 90 to 226 °C is attributed to the loss of coordinated water molecules, it starts to lose H_2L^{2-} ligands as a result of thermal decomposition above 230 °C and shows the decomposition of **3**. Compound **4** reveals a first weight loss from 30 to 197 °C, corresponding to the releasing of two lattice and two coordinated water molecules, and then another four coordinated water molecules and organic L^{4-} ligands decompose from 220 to 680 °C. Compound **5** gradually loses free waters, coordinated water molecules, phen and L^{4-} ligands with increasing temperature, matching with the fully decomposition above 250 °C (Fig. S2). The results indicate that the different structures of **1**–**5** as well as diverse coordination environment of metal ions have profound effects on the overall framework rigidity and thermal stability.

In order to check the phase purity of **1**, the X-ray powder diffraction (XRPD) pattern was checked at room temperature. As shown in Fig. S3, most peak positions of simulated and experimental patterns are in well agreement with each other. And the differences in intensity may be due to the preferred orientation of the crystalline powder sample.

3.7. Magnetic property

The variable-temperature magnetic susceptibility of **1** is carried out at an applied field of 1000 Oe in the temperature range of 2–300 K, as shown in the Fig. 5. At 300 K, the experimental $\chi_M T$ value is 8.56 $cm^3\ K\ mol^{-1}$, which is slightly lower than the spin-only value (8.76 $cm^3\ K\ mol^{-1}$, $S = 5/2$) of Mn^{2+} ions. With lowering the temperature, $\chi_M T$ value gradually decreases, which indicates an antiferromagnetic interactions of Mn^{2+} ions in **1**. Temperature dependence of the reciprocal susceptibility ($1/\chi_M$) well obeys the Curie–Weiss law ($\chi_M = C/(T-\theta)$) above 8 K with $\theta = -9.13$ K, $C = 9.68\ cm^3 K\ mol^{-1}$. The negative θ value also reveals in the presence of antiferromagnetic interactions of Mn^{2+} ions.

The distances between two adjacent Mn^{2+} ions in a zigzag chain are 4.2988 and 4.8516 Å, respectively, and the distance of Mn^{2+} ions between two adjacent chains is 9.8312 Å. Therefore, the magnetic interactions of **1** are quantitatively evaluated with similar to the binuclear Mn(II) complex system [28], the experimental magnetic data can be properly fitted using the following equation.

$$\chi_M = \frac{2Ng^2\beta^2}{kT} \times \frac{55e^{30J/kT} + 30e^{20J/kT} + 14e^{12J/kT} + 5e^{6J/kT} + e^{2J/kT}}{11e^{30J/kT} + 9e^{20J/kT} + 7e^{12J/kT} + 5e^{6J/kT} + 3e^{2J/kT} + 1}$$

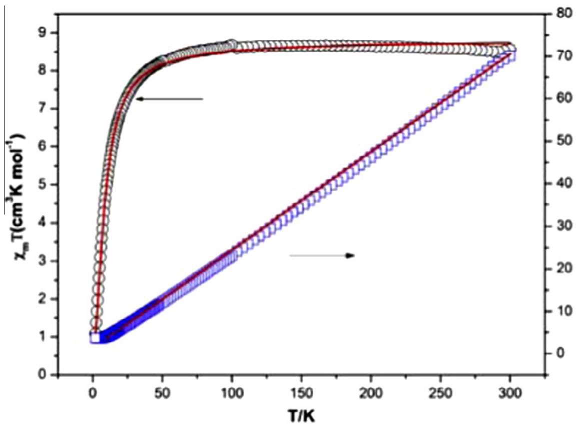

Fig. 5. Temperature dependence of the $\chi_M T$ and $\chi_M{}^{-1}$ curve for complex **1**.The red lines represent the best fit to the fitted equation in the text and the Curie–Weiss law, respectively. (For interpretation of color in Fig. 5, the reader is referred to the web version of this article.)

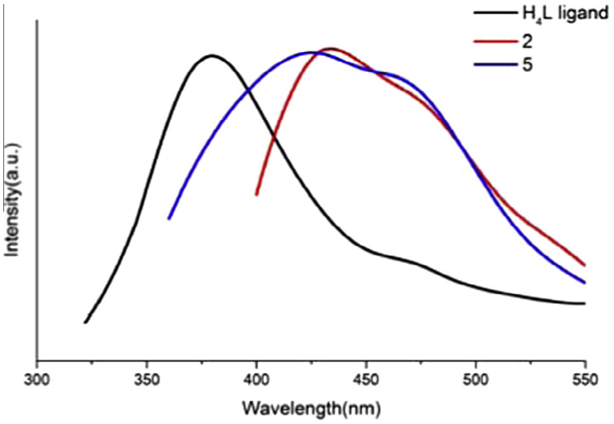

Fig. 6. Photoluminescence spectra of **2**, **5** and H_4L ligand in the solid state at room temperature.

The least-squares analysis of magnetic susceptibility data leads to $J = -0.68\ cm^{-1}$, and $g = 2.0$. The smaller negative J value suggests that weak antiferromagnetic interactions between the adjacent Mn^{2+} ions.

3.8. Photoluminescence properties

As shown in Fig. 6, the emission spectra of the H_4L ligand, **2** and **5** were examined in the solid state at room temperature. Emission of the H_4L ligand was observed with a maximum emission peak at 380 nm ($\lambda_{ex} = 300$ nm), which could be attributed to the transition of $\pi^* \rightarrow \pi$ or $\pi^* \rightarrow$ n of the ligand; the photoluminescent peak of phen is located at 381, 416 and 439 nm ($\lambda_{ex} = 350$ nm).[29] **2** exhibits a broad emission band at 434 nm ($\lambda_{ex} = 382$ nm), which is red-shifted 54 nm in comparing with that of the H_4L ligand. For **5**, a broad emission band at 425 nm ($\lambda_{ex} = 343$ nm) was observed, which is red-shifted 45 nm compared with that of the H_4L ligand. These results may be assigned to a ligand-to-metal charge transfer of **2** and **5** (LMCT).

4. Conclusions

Five transition metal coordination compounds using a semirigid tetracarboxylic acid have been prepared by the hydrothermal method. Compounds **1** and **2** are isostructural and exhibit two-dimensional layered structures. Compound **3** displays a mononuclear unit and **4**–**5** show the dinuclear structures, respectively. The magnetic property of **1** was exploited, which reveals in the presence of an antiferromagnetic interactions between Mn(II) ions. The photoluminescent properties of **2** and **5** were investigated, which could be assigned to a ligand-to-metal charge transfer.

Acknowledgements

This work is financially supported by the National Natural Science Foundation of China (No. 21361017), Inner Mongolia Natural Science Foundation of China (No. 2012MS0214) and the Scientific and Technological Key Research Project of Inner Mongolia Colleges & Universities (NJZZ12012).

Appendix A. Supplementary material

CCDC No. 918037 for **1**, 918036 for **2**, 918038 for **3**, 918039 for **4**, 918040 for **5**, which can be obtained from the Cambridge Crystallographic Data Centre free of charge via www.ccdc.cam.ac.uk/data_request/cif. Supplementary data associated with this article can be found, in the online version, at http://dx.doi.org/10.1016/j.ica.2013.08.022.

References

[1] (a) O.M. Yaghi, H.L. Li, C. Davis, D. Richardson, T.L. Groy, Acc. Chem. Res. 31 (1998) 474;
(b) J. Kim, B.L. Chen, T.M. Reineke, H.L. Li, M.D.B. Eddaoudi, J. Am. Chem. Soc. 123 (2001) 8239;
(c) R.Q. Zhong, R.Q. Zou, M. Du, T. Yamada, G. Maruta, S. Takeda, Q. Xu, Dalton Trans. (2008) 2346.
[2] J.R. Long, O.M. Yaghi, Chem. Soc. Rev. 38 (2009) 1213.
[3] H.C. Zhou, J.R. Long, O.M. Yaghi, Chem. Rev. 112 (2012) 673.
[4] (a) Q.R. Fang, G.S. Zhu, M. Xue, Q.L. Zhang, J.Y. Sun, X.D. Guo, S.L. Qiu, S.T. Xu, P. Wang, D.J. Wang, Y. Wei, Chem. Eur. J. 12 (2006) 3754;
(b) K.Z. Shao, Y.H. Zhao, Y.Q. Lan, X.L. Wang, Z.M. Su, R.S. Wang, CrystEngComm. 13 (2011) 889.
[5] (a) S.L. Li, Y.Q. Lan, J.F. Ma, J. Yang, G.H. Wei, L.P. Zhang, Z.M. Su, Cryst. Growth Des. 8 (2008) 675;
(b) Z. Shi, G. Li, L. Wang, L. Gao, X. Chen, J. Hua, S. Feng, Cryst. Growth Des. 4 (2003) 25;
(c) F. Dai, S. Gong, P. Cui, G. Zhang, X. Qiu, F. Ye, D. Sun, Z. Pang, L. Zhang, G. Dong, C. Zhang, New J. Chem. 34 (2010) 2496.
[6] X. Zhu, H.Y. Ge, Y.M. Zhang, B.L. Li, Y. Zhang, Polyhedron 25 (2006) 1875.
[7] M.L. Tong, B.H. Ye, J.W. Cai, X.M. Chen, S.W. Ng, Inorg. Chem. 37 (1998) 2645.
[8] C.Y. Su, Y.P. Cai, C.L. Chen, M.D. Smith, W. Kaim, H.C.Z. Loye, J. Am. Chem. Soc. 125 (2003) 8595.
[9] X.H. Bu, Y.B. Xie, J.R. Li, R.H. Zhang, Inorg. Chem. 42 (2003) 7422.
[10] X.R. Meng, Y.L. Song, H.W. Hou, H.Y. Han, B. Xiao, Y.T. Fan, Y. Zhu, Inorg. Chem. 43 (2004) 3528.
[11] M. Du, X.H. Bu, Y.M. Guo, H. Liu, S.R. Batten, J. Ribas, T.C.W. Mak, Inorg. Chem. 41 (2002) 4904.
[12] Z.G. Guo, R. Cao, X.J. Li, D.Q. Yuan, W.H. Bi, X.D. Zhu, Y.F. Li, Eur. J. Inorg. Chem. 5 (2007) 742.
[13] (a) X.L. Wang, C. Qin, E.B. Wang, Y.G. Li, Z.M. Su, Chem. Commun. 43 (2005) 5450;
(b) R.Q. Zou, R.Q. Zhong, M. Du, T. Kiyobayashi, Q. Xu, Chem. Commun. (2007) 2467.
[14] (a) Q. Li, W. Zhang, O.S. Miljanic, C.B. Knobler, J.F. Stoddart, O.M. Yaghi, Chem. Commun. 46 (2010) 380;
(b) J. An, S.J. Geib, N.L. Rosi, J. Am. Chem. Soc. 132 (2010) 38;
(c) Q. Yue, Q. Sun, A.L. Cheng, E.Q. Gao, Cryst. Growth Des. 10 (2010) 44;
(d) A. Lan, K. Li, H. Wu, L. Kong, N. Nijem, D.H. Olson, T.J. Emge, Y.J. Chabal, D.C. Langreth, M. Hong, J. Li, Inorg. Chem. 48 (2009) 7165;
(e) C. Marchal, Y. Filinchuk, D. Imbert, J.C.G. Bunzli, M. Mazzanti, Inorg. Chem. 46 (2007) 6242.
[15] F. Dai, J. Dou, H. He, X. Zhao, D. Sun, Inorg. Chem. 49 (2010) 4117.
[16] (a) Z. Guo, R. Cao, X. Wang, H. Li, W. Yuan, G. Wang, H. Wu, J. Li, J. Am. Chem. Soc. 131 (2009) 6894;
(b) T.F. Liu, J. Lü, Z. Guo, D.M. Proserpio, R. Cao, Cryst. Growth Des. 10 (2010) 1489;
(c) T.F. Liu, J. Lu, X. Lin, R. Cao, Chem. Commun. 46 (2010) 8439;
(d) Z.J. Lin, T.F. Liu, B. Xu, L.W. Han, Y.B. Huang, R. Cao, CrystEngComm. 13 (2011) 3321;
(e) T.F. Liu, J.A. Lu, C.B. Tian, M.N. Cao, Z.J. Lin, R. Cao, Inorg. Chem. 50 (2011) 2264.
[17] (a) Y.W. Lin, B.R. Jian, S.C. Huang, C.R. Huang, K.F. Hsu, Inorg. Chem. 49 (2010) 2316;
(b) P. Lama, A. Aijaz, S. Neogi, L.J. Barbour, P.K. Bharadwaj, Cryst. Growth Des. 10 (2010) 3410.
[18] W.T. Yang, M. Guo, F.Y. Yi, Z.M. Sun, Cryst. Growth Des. 12 (2012) 5529.
[19] (a) S.B. Ren, L. Zhou, J. Zhang, Y.L. Zhu, Y.Z. Li, H.B. Du, X.Z. You, CrystEngComm. 12 (2010) 1635;
(b) L.L. Liang, S.B. Ren, J. Zhang, Y.Z. Li, H.B. Du, X.Z. You, Cryst. Growth Des. 10 (2010) 1307.
[20] G.B. Li, J.M. Liu, Y.P. Cai, C.Y. Su, Cryst. Growth Des. 11 (2011) 2763.
[21] J. Yang, J.F. Ma, Y.Y. Liu, S.R. Batten, CrystEngComm. 11 (2009) 151.
[22] L.H. Cao, H.Y. Li, S.Q. Zang, H.W. Hou, Cryst. Growth Des. 9 (2012) 4299.
[23] X.L. Zhang, Y.T. Li, J. Zhang, J.J. Xiao, Y.F. Duan, M.L. Fu, H.Y. Sun, J. Hebei Acad. Sci. 24 (2007) 63.
[24] (a) G.M. Sheldrick, Acta Crystallogr., Sect. A 64 (2008) 112;
(b) G.M. Sheldrick, SHELXL-97, Program for Crystal Structures Refinement, University of Göttingen, Germany, 1997.
[25] (a) Z.M. Sun, F.Y. Yi, Cryst. Growth Des. 12 (2012) 5695;
(b) L.Y. Wang, X.H. Chang, J.H. Qin, L.F. Ma, J.G. Wang, Cryst. Growth Des. 12 (2012) 4652.
[26] (a) C.H. Yang, C.M. Chou, G.H. Lee, C.C. Wang, Inorg. Chem. Commun. (2003) 135;
(b) A.J. Blake, S.J. Hill, P. Hubberstey, W. Li, J. Chem. Soc., Dalton Trans. (1997) 913;
(c) C.C. Wang, C.H. Yang, G.H. Lee, Eur. J. Inorg. Chem. (2006) 820.
[27] (a) L.Y. Wang, X.H. Chang, J.H. Qin, L.F. Ma, J.G. Wang, Cryst. Growth Des. 12 (2012) 4651;
(b) S.Q. Zang, L.H. Cao, R. Liang, H.W. Hou, C.W. Mak, Cryst. Growth Des. 12 (2012) 1834.
[28] L.F. Ma, L.Y. Wang, Y.Y. Wang, M. Du, J.G. Wang, CrystEngComm. 11 (2009) 115.
[29] S.Q. Zhang, F.L. Jiang, M.Y. Wu, J. Ma, Y. Bu, M.C. Hong, Cryst. Growth Des. 12 (2012) 1452.